Large Eddy Simulation Workshop on Smooth-Body Separation

Johan Larsson, Robert Baurle, Christoph Brehm, Daniel Garmann,
Ivan Bermejo-Moreno, Marshall Galbraith, David Gonzalez,
Donald Rizzetta and Pramod Subbareddy

February 24, 2021

1 Introduction

This document describes the main test case for the workshop on smooth-body separation to be held at the AIAA SciTech meeting in January 2022. The focus of the workshop is on the use of LES methods and its many variants to accurately predict separated flows, particularly at high Reynolds numbers.

The test case described here is based on an experiment at the University of Notre Dame, but deviates from the experiment in several important ways – most importantly, by using a narrow spanwise periodic domain. The reason for deviating from the experiment is to keep the computational cost to a level where most research groups can participate, and to enable careful grid convergence studies. To explore the ability of WMLES (of all kinds, including wall-stress models and hybrid LES/RANS models) to accurately predict smooth body separation, comparisons will also be made between WMLES and wall-resolved LES (WRLES), as well as between different WMLES methods.

This document describes two different but connected test cases: (a) the complete smooth body separation case (also referred to here as the "ramp case"), and (b) a flat plate case used both to ensure that the incoming boundary layer matches the reference data, and to serve as a baseline verification test case.

2 Simulation Strategy

The computational domains for the two cases are shown in Fig. 1. The reference conditions for the incoming boundary layer (to be discussed in section 3) are defined at a location $x_{\mathrm{BL}} = -0.62L$, where $x = 0$ is the beginning of the ramp and L is the length of the ramp. As different CFD solvers will use different inflow turbulence generation techniques and different outflow damping strategies, each participant must choose: (i) how to generate inflow turbulence and what inflow profiles to prescribe, (ii) a suitable development length L_{dev}, and (iii) an appropriate outflow length L_{out}.

The choice of inflow conditions (profiles, turbulence parameters, etc.), and the choice of inflow development length, L_{dev}, will require some trial-and-error, which is easiest and cheapest to perform in a separate flat plate computation (i.e., without the ramp). The recommended simulation strategy is, therefore, to:

1. Run the zero-pressure gradient flat plate case in a way that makes sure that the boundary layer at station x_{BL} is both fully developed and matches the reference conditions. This will likely require multiple runs, adjusting the inflow condition and the development length until sufficient agreement with the reference data is achieved.

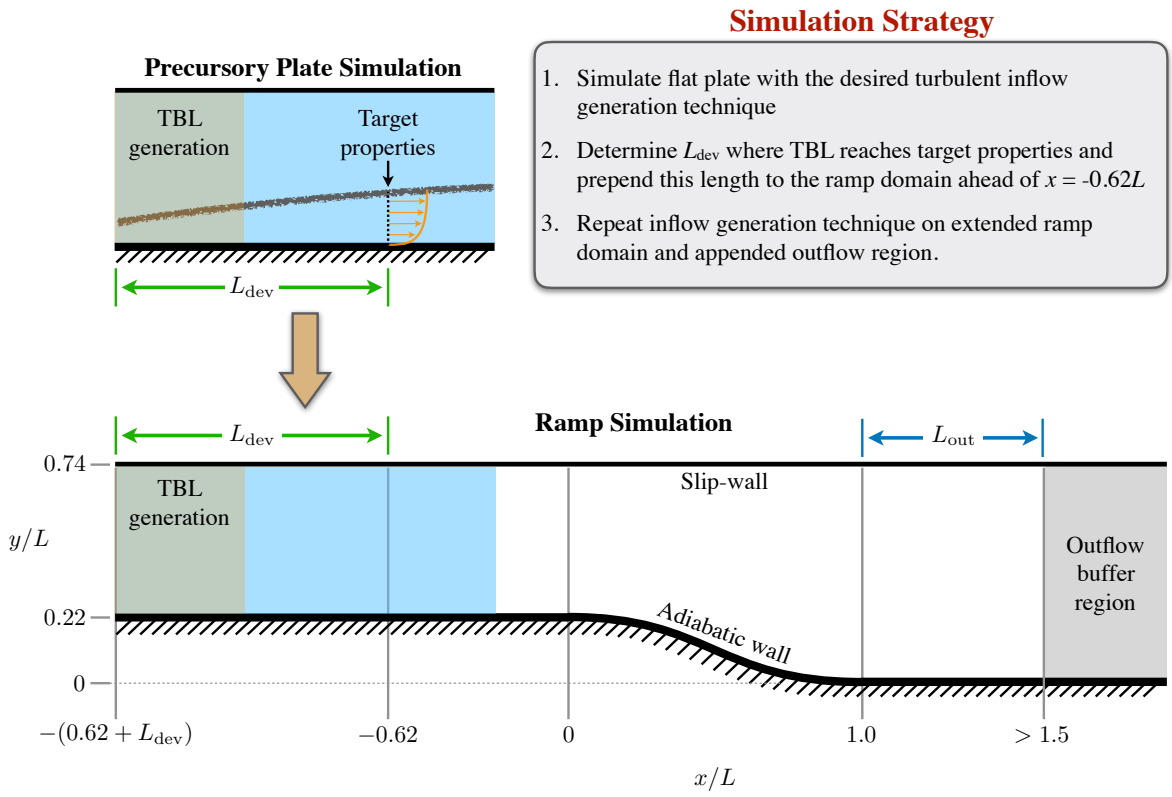

Figure 1: Computational domains for both the full ramp (lower) and the auxiliary flat plate (upper).

2. Use the final inflow conditions and development length from the flat plate test case for simulations of the full ramp geometry.

Note that the inflow parameters may have to be tuned for each grid, especially on the coarser ones. The official policy is that the boundary layer should have the desired characteristics at the $x_{\mathrm{BL}} = -0.62L$ station in the flat plate domain *for each grid*, which will then enable comparisons of results in the separated flow region on different grids knowing that they had the same incoming boundary layer.

3 Flow Conditions

The Reynolds number is defined based on the ramp length L as $Re_L = U_\infty L/\nu_\infty$, where the "$\infty$" subscript indicates the undisturbed potential flow above x_{BL}. The workshop will cover three different Reynolds numbers, at $Re_L = 3 \cdot 10^5$ (referred to as "low"), $Re_L = 1 \cdot 10^6$ ("medium"), and $Re_L = 3 \cdot 10^6$ ("high").

The organizing committee will provide WRLES for the first 2 conditions (which could be viewed as reference data).

Participants can choose to compute cases at any or all of these conditions. Note that the three different Reynolds numbers approximately correspond to: $Re_\delta = 9600$, $Re_\theta \approx 930$ and $Re_\tau \approx 450$ (for the "low" case); $Re_\delta = 32000$, $Re_\theta \approx 3100$ and $Re_\tau \approx 1300$ ("medium"); and $Re_\delta = 96000$, $Re_\theta \approx 9300$ and $Re_\tau \approx 3700$ ("high") which are all based on δ, θ, τ at x_{BL}.

Preliminary calculations by the organizing team show that the boundary layer is affected by the ramp quite far upstream, including at the reference location x_{BL}. Therefore, the state of the boundary layer at x_{BL} is not the same in the two domains. For all three Reynolds numbers, the targeted boundary layer thickness at x_{BL} is specified *in the flat plate domain*; it will then be somewhat thinner in the ramp domain. The boundary layer thickness at x_{BL} in the flat plate domain should be $\delta_{\mathrm{BL,flat\,plate}}/L = 0.032$ on every grid and at every Reynolds number, where δ is defined as the distance where the mean streamwise velocity becomes equal to 99% of U_∞.

4 Geometry

The computational domains for both the full ramp geometry and the auxiliary flat plate are shown in Fig. 1. Note that the geometry is defined by the numbers in the figure, and not by the experimental reference.

The ramp geometry is defined by a fifth-order polynomial with zero first and second derivatives at the ends following the experimental setup in Simmons *et al.* (2017, 2018):

$$\frac{y}{L} = \frac{H}{L}\left[1 - 10\left(\frac{x}{L}\right)^3 + 15\left(\frac{x}{L}\right)^4 - 6\left(\frac{x}{L}\right)^5\right], \tag{1}$$

where the ramp begins at $(x, y) = (0, H)$ and the height-to-length ratio of the ramp is $H/L = 0.22$. The top boundary of the computational domain should be treated as a slip or inviscid wall, i.e., impermeable but allowing for slip. A relatively narrow computational domain in the spanwise direction with $L_z = 0.128L$ was chosen to keep the computational cost low. The domain is wide enough to maintain a fully turbulent boundary layer but not sufficiently wide to reproduce truly realistic separated flow; however, since all participants will use the same spanwise domain size, meaningful comparisons will be possible anyway.

The computational domain for the turbulent flat plate boundary layer computations is shown in Fig. 1. For the the flat plate and ramp computations, the distance L_{dev} from the inflow to the boundary layer assessment station at $x_{\mathrm{BL}}/L = -0.62$ must be kept identical. In addition, the height of the domains must be identical, and the top boundary condition must be a slip wall in both domains.

The "useful" part of the domain should extend a distance $L_{\mathrm{out}} = 3L$ beyond the end of the ramp, i.e., up to location $x_{\mathrm{out}} = 4L$ (ignore the ">1.5" in Fig. 1, this value should be at least 4). Participants can then choose to extend this domain however they like, including with grid stretching, depending on what type of outflow boundary condition they use. For example, any sponge layer should start after $x_{\mathrm{out}} = 4L$.

5 Grids

Robert Baurle of NASA Langley has generated a whole set of grids that are available for download at `https://drive.google.com/drive/folders/1MAex7JM3T1j7hGveml-6UwCJM0jMi1ND?usp=sharing`. The Google drive directory contains a `README` file that describes the grids and the file naming convention.

There are four "families" of grids, suitable for wall-stress models at all 3 Reynolds numbers (one family) and hybrid LES/RANS approaches at each Reynolds number (three families). Each family has 6 different grids with increasing resolution, going from very coarse to very fine. The different families have identical grids in the streamwise direction, with nominally uniform grid-spacing over the full length of the ramp that is then very gently stretched towards the inlet and outlet. In

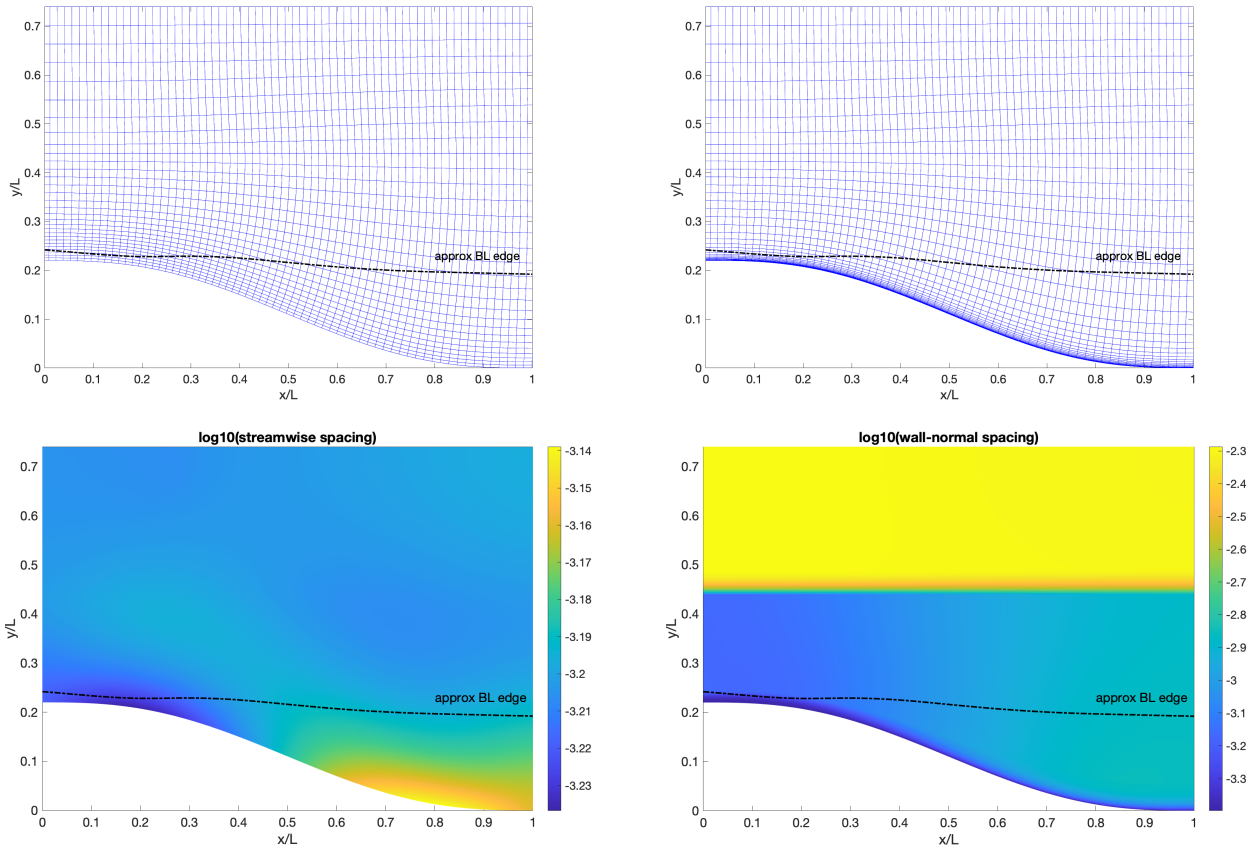

Figure 2: Visualization of the grids, showing every 4th grid line for the coarsest grids suited to wall-stress models (top left) and hybrid LES/RANS (top right), and contours of the grid-spacings (bottom).

the wall-normal direction, the grids for wall-stress models are designed approximately following the guidelines of Larsson *et al.* (2016), with uniform refinement everywhere between grid levels. The grids for hybrid LES/RANS methods are designed to have a constant y_1^+ on all grid levels to avoid an overly limiting time-step requirement in compressible codes. Note that the latter grids use a higher rate of stretching in the wall-normal direction (7.5% compared to a few percent) in order to closely represent what people do in practice. The grids are shown in Figs. 2 and 3.

The grids are 2D grids covering the main part of the domain; participants then need to extrude the grids in the spanwise direction to create 3D grids, and also towards the inflow and outflow in order to create the correct development length L_{dev} and any outflow sponge length that is required. A Fortran program `extrude.f90` has been provided to perform this grid extrusion.

The grids for the flat plate case can be generated in at least two different ways. The first is to use the `extrude.f90` code and save only the inflow domain as a separate grid. The second is for participants to read the y-coordinates for each grid in the respective files (named "`*.ycoords_before_ramp`") and then use these to generate their own grids.

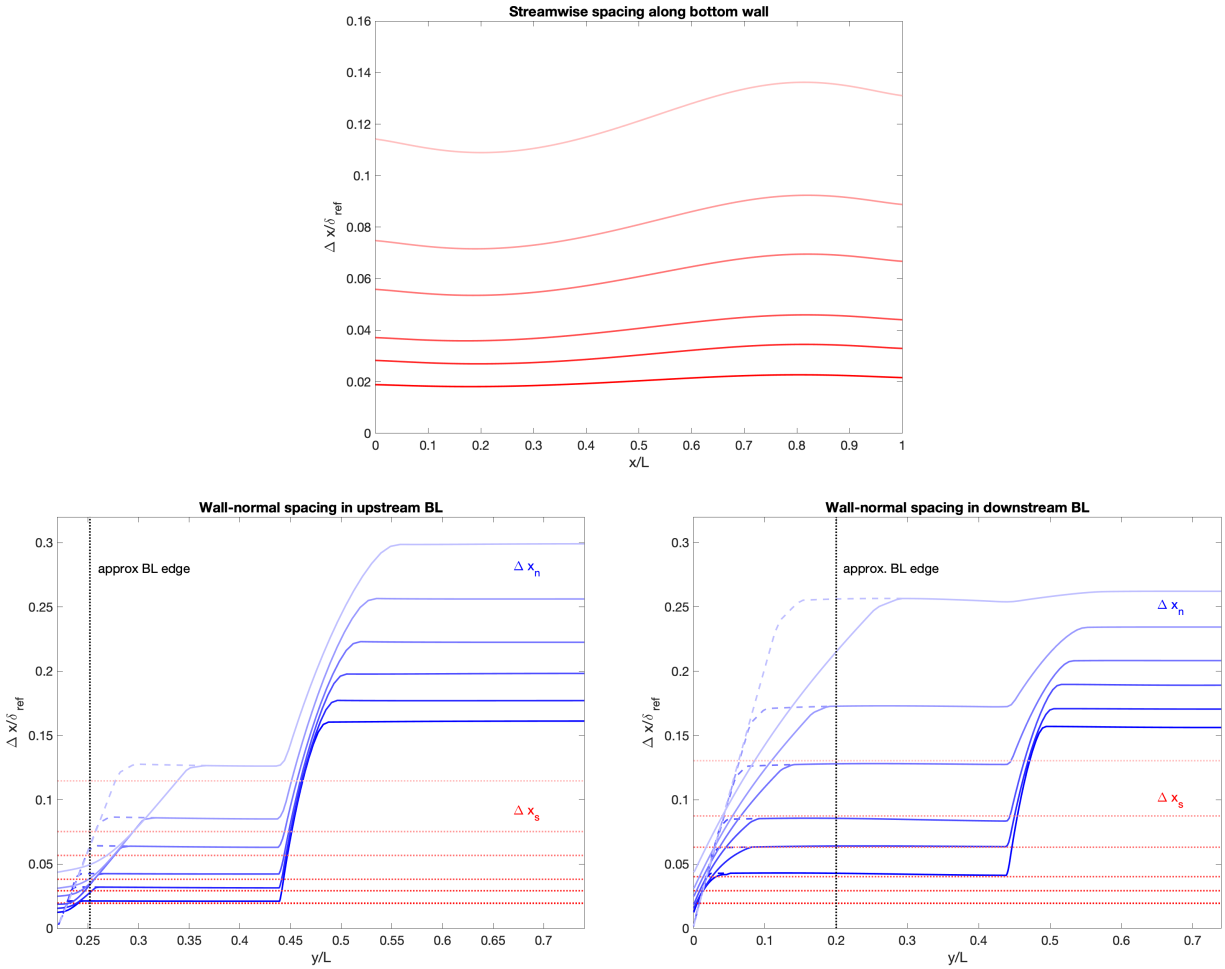

Figure 3: Grid-spacings along lines for all 6 levels of refinement. Streamwise spacing (top) and wall-normal spacing in the upstream (bottom left) and downstream (bottom right). The latter two plots show the streamwise grid-spacing as dotted red lines for reference. Note the different wall-normal grid-spacings for the wall-stress grids (solid) and hybrid LES/RANS grids (dashed).

6 Results and Submission

As we approach the workshop, participants will submit their results in a standardized format and the organizing committee will then produce a joint comparison between all submissions for each Reynolds number case. The exact data to be submitted, and in which format, will be arrived at in participant telecons during 2021. Having said that, it will include:

- Mean velocity and Reynolds stress profiles in the flat plate domain, at x_{BL} and at a location about 3δ downstream of it. Comparing the two will enable an assessment of how fully developed the flow has become. Comparing different submissions at x_{BL} will enable a comparison of how different the incoming boundary layers are, which will be an important item when comparing the separated flow.

- Mean velocity and Reynolds stress profiles in the ramp domain at x_{BL}. This will further enhance our ability to understand the differences in the incoming boundary layers between different submissions and different grids.

- Skin friction or wall shear stress on the lower wall as a function of x, to judge the extend of the separated flow region.
- Mean velocity and Reynolds stress profiles at select locations before, through, and after the separation bubble. Whether to collect this data along vertical lines (after interpolation) or along grid lines (on the organizer-generated grids) has yet to be determined.

In addition to the flow field data listed above, we also envision some comparison of computational cost. This is of course difficult to do in a fair/meaningful manner, but the number of core-hours and the number of time steps per characteristic time L/U_∞ would be informative (and should of course be interpreted judiciously, as everything else).

7 Sensitivity studies

Participants are encouraged to perform sensitivity studies on relevant parameters, including the averaging time (measuring the convergence of the averages) and the spanwise domain size (say, testing with 50% or 100% larger domain size). One item that may be of particular interest is the wall-normal stretching ratio, since common practice seems to be to use higher stretching in hybrid LES/RANS than wall-stress models.

The workshop is meant as a learning experience for all participants, and should be approached as such.

References

Larsson, J., Kawai, S., Bodart, J. & Bermejo-Moreno, I. 2016 Large eddy simulation with modeled wall-stress: recent progress and future directions. *JSME Mech. Eng. Reviews* **3**.

Simmons, D. J., Thomas, F. O. & Corke, T. C. 2017 Benchmark smooth body flow separation experiments. AIAA Paper 2017-4128.

Simmons, D. J., Thomas, F. O. & Corke, T. C. 2018 A smooth body, large-scale flow separation experiment. AIAA Paper 2018-0572.